JOURNAL OF MECHANICS OF CONTINUA AND MATHEMATICAL SCIENCES
www.journalimcms.org

ISSN (Online) : 2454 -7190 Vol.-20, No.-2, February (2025) pp 128 - 141 ISSN (Print) 0973-8975

THE INFLUENCE OF MOMENTUM AND CONCENTRATION SLIP BOUNDARY CONDITIONS ON A FERROMAGNETIC DIPOLE WITH RADIATION, THERMOPHORESIS, AND BROWNIAN MOTION

Nagagopiraju Vullam[1], Jupudi Lakshmi Rama Prasad[2], [3]M. Aruna Kumari, Ramesh Adireddy[4], Y. Subba Rao[5], U. S. B. K. Mahalaxmi[6] R. Anil Kumar[7] G. Dharmaiah[8], Desamala Prabhakar Rao[9] Sarala Patchala[10]

[1]Department of CSE, Chalapathi Institute of Engineering and Technology Guntur, Andhra Pradesh, Guntur dist-522034, India.

[2]Department of Mathematics, P. B. Siddhartha College of Arts and Science Vijayawada, A. P., India.

[3]Dept.of Mathematics, KKR&KSR Institute of Technology & Sciences Vinjanampadu, Guntur, India.

[4,6] Department of Electrical and Electronics Engineering, Aditya University Surampalem, India.

[5]Department of Mechanical Engineering, Aditya University, Surampalem India.

[7]Department of Electronics and Communication Engineering, Aditya University Surampalem, India.

[8]Dept of Mathematics, Narasaraopet Engineering College, Yellamanda, India.

[9]Associate Professor, Department of ECE, Chalapati Institute of Technology Mothadaka, Guntur, India.

[9]Associate Professor, Dept. of ECE, KKR&KSR Institute of Technology & Sciences, Vinjanampadu, Guntur, India.

Email: [1]gopi.raju524@gmail.com, [2]jlrprasad@gmail.com
[3]arunakumaridarsanapu@gmail.com, [4]rameshadireddy007@gmail.com
[5]subbaraoyarrapragada@gmail.com, [6]aumahalakshmi@gmail.com
[7]anidecs@gmail.com, [8]dharma.g2007@gmail.com, [9]prabhakardesamal@gmail.com
[10]saralajntuk@gmail.com

Corresponding Author: **M. Aruna Kumari**

https://doi.org/10.26782/jmcms.2025.02.00011

(Received: November 18, 2024; Revised: January 24, 2025; Accepted: February 08, 2025)

Abstract

A magnetic dipole effects nonlinear thermal radiation from ferromagnetic liquid when stretched provinces are analyzed numerically utilizing various parameters pertinent to the problem. Ferrofluid will undergo a phase shift and become magnetic when it is in a magnetic field. This technique is useful in various fields, including electronics, loudspeakers, and materials research. This research aimed to gain further knowledge about the one-of-a-kind continual flow of ferrofluids via permeable medium, including Brownian and thermophoresis influences. Ordinary differential equations may be generated using the appropriate similarity transformation. After that, the equations are solved by using the approach known as bvp4c. Calculations are carried out to obtain the results of physical parameters with non-dimension quantities. The effects of velocity, temperature, and concentration, as well as the applications of these factors, are shown graphically. The velocity is affected in various ways by two factors, namely, the ferromagnetic parameter and the distance. The concentration is increased due to both the thermophoretic and Brownian variables. The frictional force rises as the ferromagnetic and Brownian motion parameters increase, yet the Sherwood and Nusselt numbers decrease throughout this process.

Keywords: *Thermo-phoresis, Brownian motion, Magnetic dipole, Radiation.*

I. Introduction

The creation of ferrofluids, a kind of intelligent substance, involves dispersing ferromagnetic particles throughout a base liquid [I]. For generations, scientific researchers have been captivated by the engineering applications of magnetic liquids. Hard diskettes, spinning X-ray tubes, propellers, and poles are just a few of the numerous uses that may be found in commercially available electrical devices [II, III]. These liquids can be found in electrical motors and high-fidelity speakers to act as heat-regulating agents. Magnetic fluid is also used in sensors, densimeters, accelerometers, pressure transducers, etc. [IV]. Alternating magnetic fluid is one method that may be employed in the medical technology field to cure cancers and tumors [V]. Ferrofluids are an excellent choice for use in the vibration-dampening systems of speakers, as well as the rotary seals found in hard drives and new motors with rotating shafts. Researchers have recently been interested in Ferrofluids because of their paramagnetic properties. Ferrofluid is beneficial in many applications for various technical fields, including microchip technology, materials science, thermodynamics, biomechatronics, aerospace engineering, and related technical fields. The pharmaceutical industry uses ferrofluid for resonance magnetic imaging. An oscillating vertical surface in a magnetic region driven by gravity might facilitate the convection of a magnetite water nanofluid, according to Seth and Mandal [VI]. Astanina et al. [VII] described ferrofluid entropy formation and convection in an open trapezoidal chamber partially filled with suspended material. An open chamber filled with various horizontal permeable blocks filled with ferrofluid was studied by Gibanov et al. [VIII]. The heat transfer of ferrofluid with a non-uniform magnetic region was investigated by Asadi et al. [IX].

There are three methods in which energy may be transferred between bodies with differing temperatures, and thermal radiation is one of them. Radiation is a process of

causing things to warm up (variation of their internal energy) by emitting electromagnetic waves. By cooling or heating this material, it can transmit radiation from ultraviolet up to far-field infrared, whose specific wavelength depends on its temperature. Radiation from nearby and distant sources constantly affects the body. Heat radiation is carried and received by chemical reactions in the transmitter, the receiver, and the medium. Using specific temperatures, a body can transfer and store heat. Using a rotating reference frame, Vedavathi et al. [X] experimented with the consequences of moving metastable high-density radiation beams and metallic nanoparticles. Radiative nondarcy nanofluid flow in convective conditions by Vedavathi et al. [XI]. Mohiddin et al. [XII] studied natural convection's MHD flow and examined how heat production and radiation affected it.

Particles in a fluid that are on the nanoscale are called a "nanofluid" [XIII],[XIV]. In addition, there are no unintended repercussions associated with working with nanoparticles, such as pressure loss, erosion, or sedimentation. Brownian motion-induced convection and consequence transfer via propagating nanoparticle routes are the most common strategies for improved heat transmission in nanofluids, according to thorough research [XV-XVIII]. They investigated several technological configurations with heat augmentation in mind.

Saeed et al. [XIX] work has been extended using the studies mentioned above to experience these kinds of consequences. By using a wide range of parameters, we explore the effects of a magnetic dipole on nonlinear thermal radiation in ferromagnetic liquid throughout a stretched province. This analysis takes place throughout the province. Along with the magnetic field, ferrofluid will experience a phase change, resulting in the fluid acquiring magnetic properties. This method may be helpful in many areas, such as electronics, research on loudspeakers, and developing new materials. As part of this inquiry, it was investigated whether and how Brownian motion and thermophoresis impact the flow of ferrofluids in porous media. An appropriate similarity transformation can be used to create ordinary differential equations (ODEs). In the following step, a technique called bvp4c is applied to solve the equations. To obtain the results of physical parameters using non-dimension quantities, calculations are performed.

II. Mathematical Formulation

The flow of a viscous magnetite ferrofluid powered by an impermeable stretched surface assumes continuous 2-D flow. Flow assumptions are: Two equivalent and opposing forces acting along the horizontal plane, also christened by the x-axis, direction perpendicular to the flow, also christened by the y-axis, are what produce the flow. With $u(x)$ velocity-related farness away from 'O', the sheet is extended. Somewhat beneath the sheet, there is a magnetic dipole. The dipole's center is situated above the y-axis, 'a' below the x-axis. Its magnetic flux is rather reliable and completely saturates the ferrofluid, pointing in the positive towards the x-direction. A set temperature T_w that is lower than the Curie temperature T_c, is maintained for the stretching sheet. Fluid essentials furthest from the wall, however, are perceived as at temperature $T = T_c$, so unable to be magnetized until they enter the thermal boundary next to the sheet and start to cool [19]. This paper considers a magnetite ferrofluid. This

fluid is viscous, incompressible, 2-D steady flow, and guided by an impermeable stretching plane. Fig.1 illustrates the physical flow of the model. The following flow assumptions are underlying:

1. By interacting two opposing forces, the axis shows the flow's x-direction. There is no flow along the y-axis.
2. A sheet stretches by varying its velocity inversely with its origin.
3. An underground magnetic dipole exists far below the sheet.
4. Magnetic saturation of positive x-direction ferrofluid spots is significant. To prevent the sheet from magnetizing, we maintained a constant temperature T_w underneath Curie temp (T_c).
5. Considering fluid components at a distance $T = T_c$.
6.

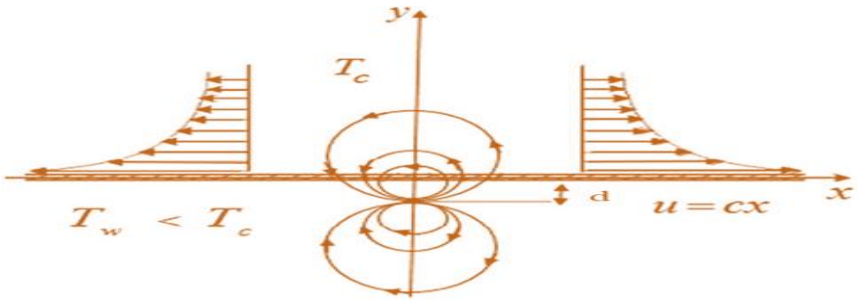

Fig.1. An illustration of the physical flow of a model.

Scalar magnetize-potential, their components, magnetic field *H* [16]:

$$V = \frac{\gamma}{2\pi}\frac{x}{x^2+(y+d)^2}, \tag{1}$$

$$H_x = -\frac{\partial V}{\partial x} = \frac{\gamma}{2\pi}\ \frac{x^2-(y+d)^2}{[x^2+(y+d)^2]^2}, \tag{2}$$

$$H_y = -\frac{\partial V}{\partial y} = \frac{\gamma}{2\pi}\frac{2x(y+d)}{[x^2+(y+d)^2]^2}, \tag{3}$$

$$\|H\| = \left\{\left(\frac{\partial V}{\partial x}\right)^2 + \left(\frac{\partial V}{\partial y}\right)^2\right\}^{\frac{1}{2}}, \tag{4}$$

From Eqs. (3) and (4) $\frac{\partial H}{\partial x} = -\frac{\gamma}{2\pi}\frac{2x}{(y+d)^4}$, (5)

$$\frac{\partial H}{\partial y} = \frac{\gamma}{2\pi}\left\{\frac{-2}{(y+d)^3} + \frac{4x^2}{(y+d)^5}\right\}. \tag{6}$$

Ferrofluid boundary layer equations follow [19, 20]:

$$u\frac{\partial u}{\partial x} + v\frac{\partial u}{\partial y} = 0, \tag{7}$$

$$u\frac{\partial u}{\partial x} + v\frac{\partial u}{\partial y} = \frac{\partial}{\partial y}\left(\mu(T)\frac{\partial u}{\partial y}\right) + \rho g\beta_t(T - T_\infty) + \frac{\lambda_0 M}{\rho}\frac{\partial H}{\partial x} - \frac{v}{K} \tag{8}$$

$$u\frac{\partial T}{\partial x} + v\frac{\partial T}{\partial y} = \frac{1}{\rho C_p}\frac{\partial}{\partial y}\left(K(T)\frac{\partial u}{\partial y}\right) - \frac{1}{\rho C_p}\frac{\partial q_r}{\partial y} - \frac{\mu_0}{\rho C_p}T\frac{\partial M}{\partial T}\left(u\frac{\partial H}{\partial x} + v\frac{\partial H}{\partial y}\right), \tag{9}$$

$$u\frac{\partial C}{\partial x}+v\frac{\partial C}{\partial y}=D_m\frac{\partial^2 C}{\partial y^2}+\frac{D_T}{T_\infty}\frac{\partial^2 T}{\partial y^2}. \tag{10}$$

Problem boundary conditions:: [19, 20]

$$u=u_w(x)+A_1\frac{\partial u}{\partial y}, v=0, T=T_w, C=C_w+K_1\frac{\partial C}{\partial y}\, at\ y=0 \tag{11}$$

$$u\to 0, T\to T_\infty, C\to C_\infty, as\ y\to\infty \tag{12}$$

The heat flux q_r and T^4 are considered from [11, 21, 22]

$$q_r=\frac{4}{3}\frac{\sigma^*}{k^*}\frac{\partial T^4}{\partial y} \tag{13}$$

and $T^4\cong 4TT_\infty^3-3T_\infty^4$ (14)

The similarity transformations are

$$\left.\begin{aligned}&\eta=\sqrt{\frac{c}{v}}y, \psi=\sqrt{cv}xf(\eta), u=\frac{\partial\psi}{\partial y}=cxf'(\eta), u=-\frac{\partial\psi}{\partial x}=-\sqrt{av}f(\eta), \theta(\eta)=\frac{T-T_\infty}{T-T_\infty},\\&\phi(\eta)=\frac{C-C_\infty}{C-C_\infty}, Pr=\frac{k}{\mu C_p}, Le=\frac{v}{D_m}, M=\frac{\sigma B_0^2}{c\rho}, T_r=\frac{16\sigma^* T_\infty^3}{3kk^*}, \lambda=\frac{c\mu^2}{\rho k(T_w-T_\infty)}, \epsilon=\frac{T_\infty}{T_w-T_\infty},\\&\beta=H^2aK(T_c-T_\infty), M=K(T_c-T), \lambda_1=\frac{Gr}{Re_x^2}, \Gamma=\frac{v}{kc}, \delta=A\sqrt{\frac{c}{v}},\\&\gamma_1=c(T_w-T_\infty), \mu(T)=\mu_0 e^{-a(T-T_\infty)}, K(T)=Ke^{\epsilon\left(\frac{T-T_\infty}{T_w-T_\infty}\right)}.\end{aligned}\right\} \tag{15}$$

The nomenclature section provides all parameters.

A dimensionless equation is

$$(1-\gamma_1\theta)[f'''-\gamma_1 f''\theta']-f'^2+ff''-\frac{2\beta\theta}{(\eta+\alpha)^4}+\theta\lambda_1-\Gamma f'=0, \tag{16}$$

$$[1+\epsilon\theta+T_r]\theta''+Pr\, f\,\theta'+\epsilon\theta'^2+(\theta+\epsilon)\left\{\left[\frac{4f}{(\eta+\alpha)^5}+\frac{2f'}{(\eta+\alpha)^4}\right]Re_x\,\beta\,\lambda-\frac{2\lambda\beta}{(\eta+\alpha)^3}f\right\}=0, \tag{17}$$

$$\phi''+Lef\phi'+\frac{Nt}{Nb}\theta''=0. \tag{18}$$

Transformed boundary conditions:

$$f'(0)=1+\delta f''(0), f=0, \theta(0)=1, \phi(0)=1+S\phi'(0)\ at\ \eta=0, \tag{19}$$

$$f'(\eta)\to 0, \theta(\eta)\to 0, \phi(\eta)\to 0\ as\ \eta\to\infty. \tag{20}$$

Physically, noteworthy quantities includes C_{f_x}, Nu, and Sh, be stated:

$$C_{f_x}Re_x^{\frac{1}{2}}=(1-\gamma_1\theta(0))f''(0), \tag{21}$$

$$Nu\,Re_x^{-\frac{1}{2}}=-\left(1+\frac{4}{3}T_r\right)\theta'(0), \tag{22}$$

$$Sh\,Re_x^{-\frac{1}{2}}=-\phi'(0). \tag{23}$$

Here $Re_x = \frac{xu_w}{\upsilon}$ refers to Reynolds number.

III. Solution Methodology

The bvp4c method numerically accounts for the resulting linked nonlinear Eqs. (16)–(18) and BCs (19)–(20). The model's numerical approach flowchart is shown below. (Fig 2).

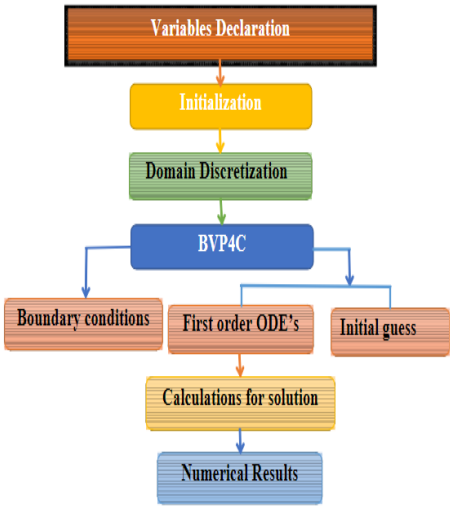

Fig. 2. Model solving flow chart.

A finite difference code known as bvp4c may be used to implement the three-stage Lobatto IIIa formula. A collocation formula like this one has a solution provided by the collocation polynomial, which is accurate to the fourth order over the whole integration interval and C1-continuous. Both the mesh selection and error management are based on the residual of the continuous solution. Collocation methods divide the integration interval into subintervals using a mesh of points. Solvers find a numerical solution to this problem by solving a global set of algebraic equations resulting from the boundary constraint as well as the combination of subinterval constraints. After that, the solver will attempt to estimate the number of errors associated with each subinterval's numerical solution.

IV. Results and Discussion

The findings from the numerical calculations are explained in physical terms. Saeed et al. [19] provide an extension of these kinds of consequences using the aforementioned sources. In the work, fixed values include $Le = \gamma_1 = \lambda_1 = \beta = \alpha = 0.5$, $\Gamma = 0.4$, $\gamma_1 = 0.5$, $Re_x = 2$, $T_r = 3$, $\delta = 0.2$, $Nt = 0.1 = 0.1$.

A study of the effects of β on velocity distribution is presented in Fig 3. When β is enhanced velocity, this is because by increasing the value of the ferromagnetic interaction parameter, the strength of the magnetic field is increased due to the existence of a direct proportion between them, and therefore, this causes disturbances to the molecules inside the fluid, which causes an increase in fluid speed. A study of the effects of α on velocity distribution is presented in Fig 4. When α is enhanced

velocity. As the distance parameter boosts, the molecules move for a longer distance, which expands the fluid's diffusion range and velocity. A study of the effects of Γ on velocity distribution is presented in Fig 5. When Γ is enhanced velocity. Physically this occurs because the magnetic permeability is directly proportional to viscosity and inversely proportional to thermal conductivity, causing an effect of fluid velocity with strengthening magnetic permeability. A study of the effects of λ_1 on velocity distribution is presented, patterns are illustrated in Fig 6. When λ_1 is enhanced, it shows an enhancement in velocity. The effect of the mixed convective parameter is inversely proportional to the Reynolds number, meaning that there is an inverse relationship between this parameter and the fluid density, i.e., that as the mixed convective parameter upsurges, the density is diminished, and thus the fluid velocity is improved. A study of the effects of γ_1 on velocity distribution is presented in Fig 7. When γ_1 is enhanced, it shows a reduction in velocity. The upsurge in the variable viscosity leads to disturbances within the particles that make up the fluid, which reduces its rapidity due to the difference in viscosity from one position to another within the fluid, which leads to an imbalance in the movement of the molecules. A study of the effects of ϵ on velocity distribution is presented in Fig 8. When ϵ is enhanced, it shows an improvement in velocity.

An impression of Pr on temperature is conferred by the scatter plot in Fig 9. Therefore, when Pr upsurges, temperature declines. An impression of Re_x on the temperature in Fig 10. When Re_x growths, the temperature improves. Increasing the density of the fluid causes the fluid to slow down and thus retains its thermal energy stored internally. A scatter plot, as shown in Fig 11, is used to analyze the impact of Tr on temperature. Therefore, as T_r growths, the temperature progresses. Physically, this occurs due to an upsurge in the internal heat energy of the fluid molecules, which in turn increases fluid temperature due to the increase in the temperature of the molecules.

Fig 12 shows the effects of Lewis's number on the concentration of the constituents. As the Lewis number increases, the concentration profiles become more uniform. This impact on the concentration of the fluid in question is caused by the direct link between the fluid's viscosity and the Lewis number. Fig 13 displays the effects of the thermophoresis parameter Nt on the concentration distribution. As Nt increases, the concentration fields get larger. The concentration distributions expand as a result of the increased concentration of nanoparticles caused by the increased thermophoresis force as Nt rises. Both the concentration distribution and the limit layer viscosity increase when the Nb concentration increases, as seen in Fig 14. Macroscopic particles in the liquid are more prone to move randomly and collide as Nb grows. Consequently, the liquid concentration will be greater. It is possible to arbitrarily reduce fluid velocity by increasing Nb.

Due to the relationship between the thermophoretic and Brownian parameters and the thermal diffusion occurring inside the fluid, an increment in the concentration of the fluid occurs with the increase of these parameters.

The Cf viscosity parameter is shown against the Lewis number in Fig 15. See Fig 16 for the radiation parameter vs. the Cf ferromagnetic parameter impact. An increase in Cf is the consequence of a larger ferromagnetic parameter. See how the Nu viscosity

parameter relates to the Lewis number in Fig 17. Increases in the viscosity parameter cause a decrease in Nu. Shown in Fig 18 are the nu ferromagnetic parameters and how they affect the radiation parameter.

Nu falls as the ferromagnetic parameter rises. Physically, with increasing temperature, the heat transport rate is diminished as a result of rising in the studied effects of the parameters governing the problem, and the Nusselt quantity is reduced. The impact of Sh thermophoresis parameter is shown in Fig 19. As the Thermophoresis parameter is adjusted upwards, the Sh is reduced. The impact of Sh on Nb is seen in Fig 20. As Nb heightens, likewise, Sh. Physically, with increasing concentration, the mass transmission rate is diminished as a result of rising in the studied effects of the parameters governing the problem, and the Sherwood number is reduced.

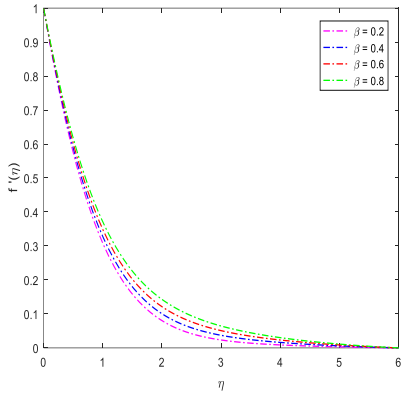

Fig. 3. Velocity at distinct values of β.

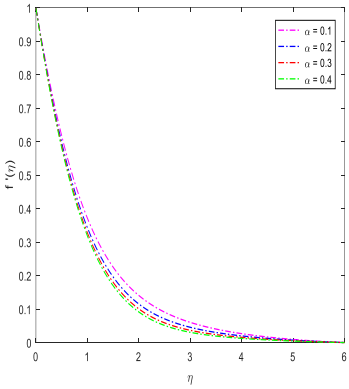

Fig. 4. Velocity at distinct values of α.

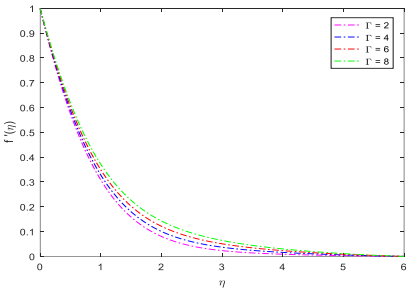

Fig. 5. Velocity at distinct values of Γ.

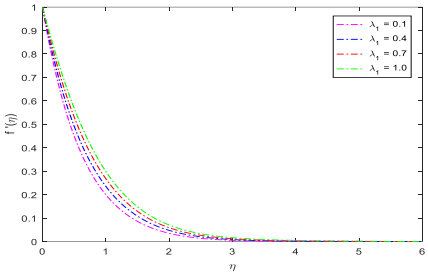

Fig. 6. Velocity at distinct values of λ_1.

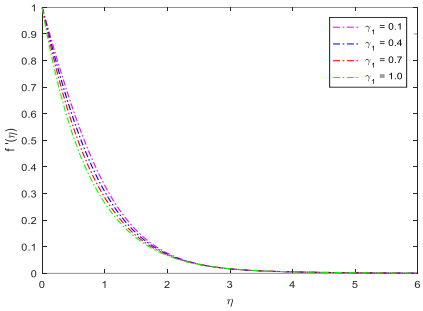

Fig. 7. Velocity at distinct values of γ_1.

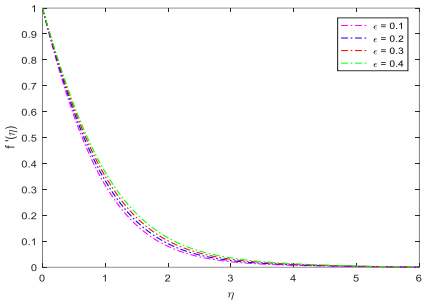

Fig. 8. Velocity at distinct values of ϵ.

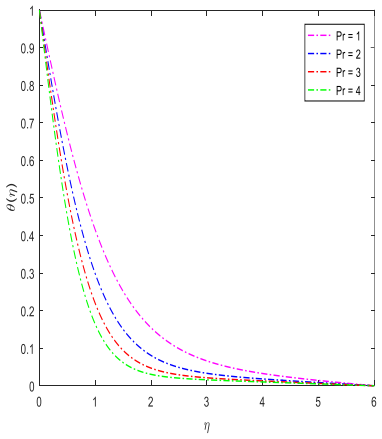

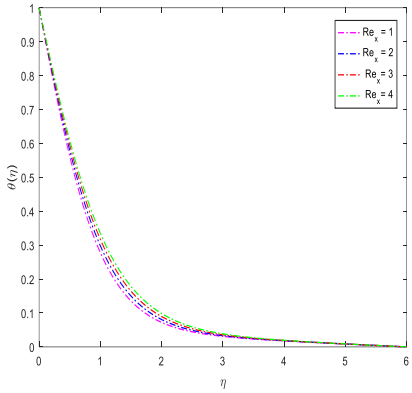

Fig.9. Temperature distinct at. different values of Pr **Fig.10**. Temperature at distinct values of Re_x.

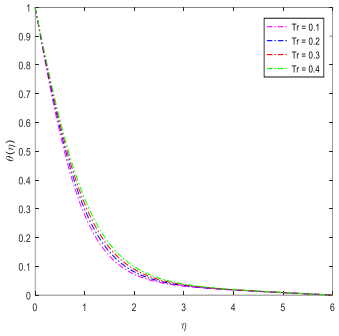

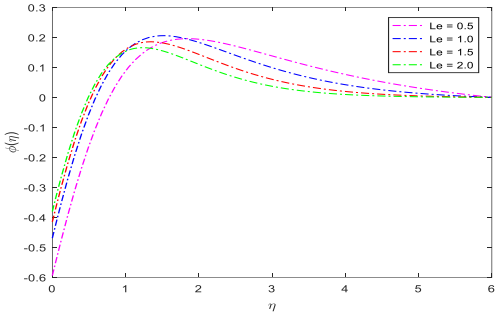

Fig.11. Temperature at. values of T_r

Fig.12. Variation of concentration at distinct distinct values of Le.

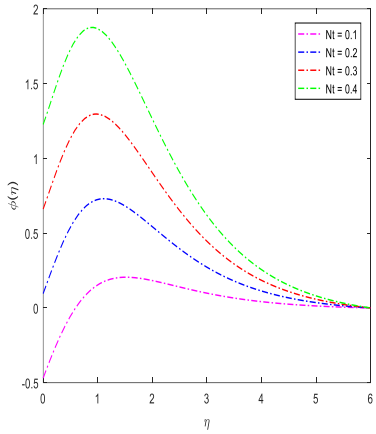

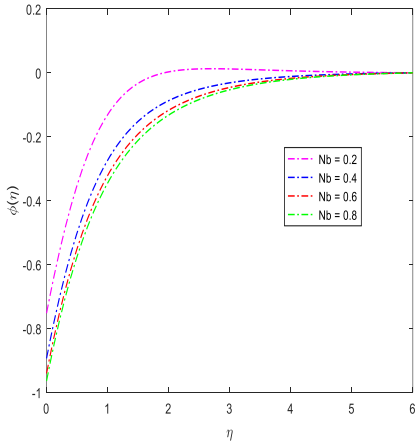

Fig.13. Variation of concentration. values of Nt

Fig.14. Variation of concentration at distinct at distinct values of Nb.

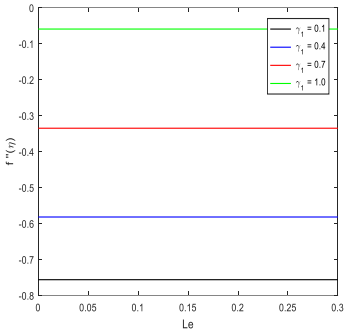

Fig.15. Presence of γ_1 on C_{f_x}. against Le

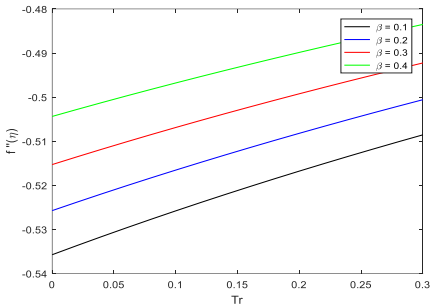

Fig16. The presence of β on C_{f_x} against T_r.

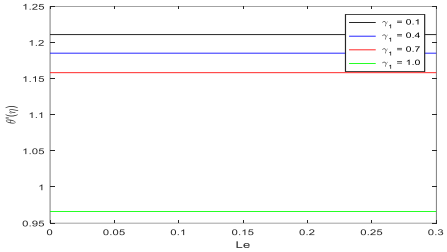

Fig 17. Presence of γ_1. on Nu against Le

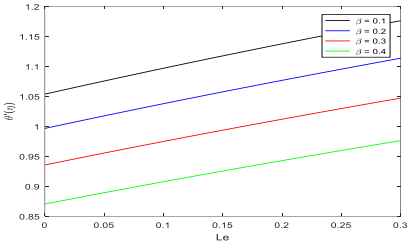

Fig18. The presence of β on Nu against T_r.

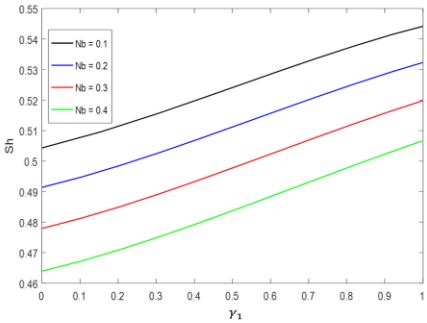

Fig 19. The presence of Nb on. Sh against γ_1

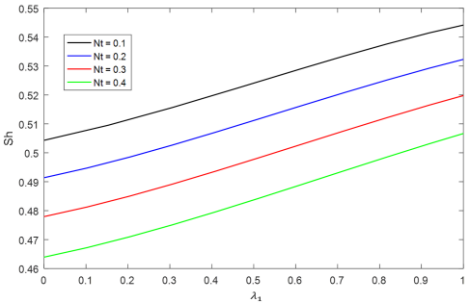

Fig20. The presence of Nt on Sh against λ_1.

Our results are good agreement with earlier published work ([19], [33]).

Pr	Ref.[19]	Ref.[33]	Current work	Error
0.70	0.453957	0.453958	0.4539575	$1x10^{-6}$
1.00	1.333333	1.333333	1.3333333	0
2.00	0.91132	0.91132	0.9113232	$1x10^{-6}$
3.00	2.509721	2.50972	2.509723	$3x10^{-6}$
10.00	4.96821	4.79682	4.96821	$2x10^{-6}$

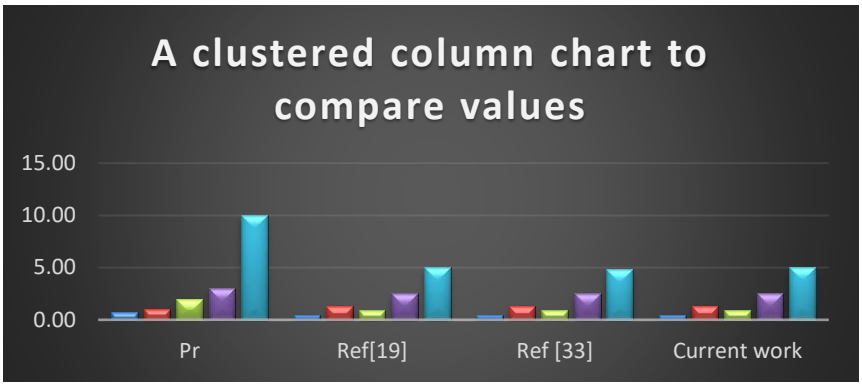

Fig. 21. A pictorial chart to compare validation

V. Conclusion-report

We numerically study, with a wide variety of important parameters, the effects of the magnetic dipole on nonlinear thermal ferromagnetic fluid throughout a stretching zone. The experiment was also conducted to get a better understanding of the peculiar steady flow of ferrofluids in porous media accompanied by Brownian motion and the effects of thermophoresis. Differential equations for ordinary differentials may be obtained by using the acceptable similarity transformation.

i. A velocity depends on two variables, distance and ferromagnetic parameter.
ii. A rising Prandtl number results in a lower thermal boundary layer thickness and temperature.
iii. Both the Nt and the Nb raise the concentration.
iv. The ferromagnetic and Brownian motion parameters are raised, and the skin friction increases, but the Sherwood and Nusselt numbers fall.

Nomenclature

x	horizantal coordinate (m)
y	vertical coordinate (m)
u	horizontal velocity (m/s)
v	vertical velocity (m/s)
T	fluid temperature inside the boundary layer (K)
T_w	temperature of the sheet (K)
T_∞	fluid temperature far away from the sheet (K)
H	magnetic field of intensity (A/m)
C_p	specific heat at constant pressure $(J\ /\ kg.K)$
C_f	skin-friction coefficient
Nu	the local Nusselt number
Sh	the local Sherwood number
D_m	mass diffusivity
k^*	the mean absorption coefficient

d	The distance between the origin and center of the magnetic dipole/distance parameter.
T_r	radiation parameter
Pr	Prandtl number
Le	Lewis number
δ	the first-order velocity slip parameter
M	magnetization (kg/s^2A)
C_w	the concentration of the fluid near the surface
$\theta(\eta)$	the dimensionless temperature
$f'(\eta)$	the dimensionless velocity
Nt	thermo-phoresis parameter
Nb	Brownian motion parameter

Greek symbols

η	similarity variable
ψ	stream function (m^2/s)
ρ	density of the fluid (kg/m^3)
μ	dynamic viscosity (kg/ms)
τ_w	wall shear stress
σ	the electrical conductivity
σ^*	the Stefen-Boltzmann constant
γ	the strength of the magnetic field
β	ferromagnetic interaction parameter
ϵ	dimensionless curie temperature
Γ	magnetic permeability (s/m^2)
α	distance parameter
γ_1	viscosity parameter
λ_1	mixed convective parameter

Conflicts of Interest

The authors declare that they have no conflict of interest exists.

References

I. Asadi, A.H. Nezhad, F. Sarhaddi, T. Keykha, “Laminar ferrofluid heat transfer in presence of non-uniform magnetic field in a channel with sinusoidal wall: a numerical study”, J. Magn. Magn. Mater. 471 (2019) 56–63. 10.1016/j.aej.2022.12.031

II. Dhanke, Jyoti Atul, K. Thanesh Kumar, Pudhari Srilatha, Kurapati Swarnalatha, P. Satish, and S. Abdul Gaffar. "Magnetohydrodynamic radiative simulations of eyring–powell micropolar fluid from an isothermal cone." International Journal of Applied and Computational Mathematics 8, no. 5 (2022): 232. 10.1007/s40819-022-01436-9

III. G. Dharmaiah, W. Sridhar, K. AL-Farhany, K. Balamurugan, F. "Ali, Non-Newtonian nanofluid characteristics over a melting wedge: A numerical study", Heat Transfer 51(5) (2022) 4620-4640. 10.1002/htj.22515

IV. H.I. Andersson, O.A. Valnes, Flow of a heated ferrofluid over a stretching sheet in the presence of a magnetic dipole, Acta Mech. 128(1) (1998) 39–47. 10.1007/bf01463158

V. K. Rafique, M.I. Anwar, M. Misiran, I. Khan, A.H. Seikh, E.-S.M. Sherif, K.S. Nisar, Brownian motion and thermophoretic diffusion consequences on micropolar type nanofluid flow with Soret and Dufour impacts over an inclined sheet: Keller-box Simulations, *Energies* 12 (2019) 4191. 10.3390/en12214191

VI. Kotha Gangadhar, Aruna Kumari, etc "Magnetization for Burgers' Fluid Subject to Convective Heating and Heterogeneous-Homogeneous Reactions" Mathematic Problem in Engineering, Febuary 2022:1-1. 10.1155/2022/2747676

VII. M. Astanina, M. Sheremet, H. Oztop, N. Abu-Hamdeh, MHD natural convection and entropy generation of ferrofluid in an open trapezoidal cavity partially filled with a porous medium, Int. J. Mech. Sci. 136 (2018) 493–502. 10.1016/j.ijmecsci.2018.01.001

VIII. N. Gibanov, M. Sheremet, H. Oztop, MHD natural convection and entropy generation in an open cavity having different horizontal porous blocks saturated with a ferrofluid, J. Magn. Magn. Mater. 452 (2018) 193–204. 10.1016/j.jmmm.2017.12.075

IX. N.A.A.M. Nasir, T. Sajid, W. Jamshed, G.C. Altamirano, M.R. Eid, F.A.A. ElSeabee, Cubic Chemical Autocatalysis and Oblique Magneto Dipole Effectiveness on Cross Nanofluid Flow via a Symmetric Stretchable Wedge, Symmetry 15(6) (2023) 1145. 10.3390/sym15061145

X. N. Vedavathi, V.S. Sajja, etc.. "Metallic nano particle effect on unsteady convective MHD flow of radiation with rotating frame of reference: A theoretical study" , AIP Conference Proceedings, AIP Publishing LLC, 2021, p. 020033. 10.1063/5.0067493

XI. G. Dharmaiah, S. Dinarvand, K. Balamurugan, "MHD radiative ohmic heating nanofluid flow of a stretching penetrable wedge: A numerical analysis", Heat Transf. 51(5) (2022) 4522-4543. 10.1002/htj.22511

XII. N. Vedavathi, G. Dharmaiah, K. Venkatadri, S.A. Gaffar, Numerical study of radiative non-Darcy nanofluid flow over a stretching sheet with a convective Nield conditions and energy activation, Nonlinear Eng. 10(1) (2021) 159-176. 10.1515/nleng-2021-0012

XIII. P. Durgaprasad, S.V.K. Varma, M.M. Hoque, C.S.K. Raju, Combined consequences of Brownian motion and thermophoresis parameters on three-dimensional (3D) Casson nanofluid flow across the porous layers slendering sheet in a suspension of graphene nanoparticles. *Neural Comput. Appl.* 31 (2018) 6275–6286. 10.1007/s00521-018-3451

XIV. N. Abbas, W. Shatanawi, T.A. Shatnawi, F. Hasan, Theoretical analysis of induced MHD Sutterby fluid flow with variable thermal conductivity and thermal slip over a stretching cylinder, AIMS Math. 8(5) (2023) 10146-10159. 10.3934/math.2023513

XV. Parige, Leela Santi, Deevi Sateesh Kumar, and Gudala Balaji Prakash. "Significance of Joule Heating and Fourier Heat Flux on the Dynamics of Ternary Hybrid Nanofluid Rotating in a Circular Porous Disk." International Journal of Heat & Technology 42, no. 5 (2024). 10.18280/ijht.420532

XVI. Raju, T. Linga, and P. Satish. "Hall and rotation effects on magnetohydrodynamics two fluids slip flow of ionized gases via parallel conduit." Heat Transfer 52, no. 7 (2023): 4829-4856. 10.1002/htj.22909

XVII. S. M. Hussain, W. Jamshed, A comparative entropy-based analysis of tangent hyperbolic hybrid nanofluid flow: Implementing finite difference method, International Communications in Heat and Mass Transfer, vol. 129, pp. 105671, 2021 10.1016/j.icheatmasstransfer.2021.10567

XVIII. Y. Lin, Y. Jiang, Consequences of Brownian motion and thermophoresis on nanofluids in a rotating circular groove: A numerical simulation, Int. J. Heat Mass Transf. 123 (2018) 569 582. 10.1016/j.ijheatmasstransfer.2018.02.103

XIX. W. Jamshed, S. U. Devi S, M. Goodarzi, M. Prakash, K. S. Nisar, M. Zakarya and A. H. Abdel-Aty, Evaluating the unsteady Casson nanofluid over a stretching sheet with solar thermal radiation: An optimal case study, Case Studies in Thermal Engineering, vol. 26, pp. 101160, 2021. 10.1016/j.csite.2021.101160

XX. W. Jamshed, K. S. Nisar, R. W. Ibrahim, T. Mukhtar, V. Vijayakumar and F. Ahmad, Computational frame work of Cattaneo-Christov heat flux effects on Engine Oil based Williamson hybrid nanofluids: A thermal case study, Case Studies in Thermal Engineering, vol. 26, pp. 101179, 2021. 10.1016/j.csite.2021.101179